Geophysical Research Letters

RESEARCH LETTER
10.1029/2019GL083699

Climate Change Increases the Potential for Extreme Wildfires

Giovanni Di Virgilio[1], Jason P. Evans[1,2], Stephanie A. P. Blake[1], Matthew Armstrong[3], Andrew J. Dowdy[4], Jason Sharples[5], and Rick McRae[6]

[1]Climate Change Research Centre, University of New South Wales, Sydney, New South Wales, Australia, [2]Australian Research Council Centre of Excellence for Climate Extremes, University of New South Wales, Sydney, New South Wales, Australia, [3]Centre for Water, Climate and Land, University of Newcastle, Newcastle, New South Wales, Australia, [4]Climate Research Section, Bureau of Meteorology, Melbourne, Victoria, Australia, [5]School of Science, University of New South Wales, Canberra, ACT, Australia, [6]Australian Capital Territory Emergency Services Agency, Canberra, ACT, Australia

Key Points:
- Significant increases in the frequency of conditions conducive to pyrocumulonimbus fires occur in November (Spring) 2060-2079 versus 1990-2009
- Atmospheric instability and dryness are better indicators of pyrocumulonimbus fire development than surface fire weather
- Locations in southeast Australia where these changes are projected to occur are identified

Supporting Information:
- Supporting Information S1

Correspondence to:
G. Di Virgilio,
giovanni@unsw.edu.au

Citation:
Di Virgilio, G., Evans, J. P., Blake, S. A. P., Armstrong, M., Dowdy, A. J., Sharples, J., & McRae, R. (2019). Climate change increases the potential for extreme wildfires. *Geophysical Research Letters*, *46*, 8517–8526. https://doi.org/10.1029/2019GL083699

Received 13 MAY 2019
Accepted 13 JUL 2019
Accepted article online 16 JUL 2019
Published online 29 JUL 2019

Abstract Pyrocumulonimbus (pyroCb) wildfires cause devastation in many regions globally. Given that fire-atmosphere coupling is associated with pyroCbs, future changes in coincident high index values of atmospheric instability and dryness (C-Haines) and near-surface fire weather are assessed for southeastern Australia using a regional climate projection ensemble. We show that observed pyroCb events occur predominantly on forested, rugged landscapes during extreme C-Haines conditions, but over a wide range of surface fire weather conditions. Statistically significant increases in the number of days where both C-Haines and near-surface fire weather values are conducive to pyroCb development are projected across southeastern Australia, predominantly for November (spring), and less strongly for December (summer) in 2060-2079 versus 1990-2009, with future C-Haines increases linked to increased 850-hPa dewpoint depression. The increased future occurrence of conditions conducive to pyroCb development and their extension into spring have implications for mitigating these dangerous wildfires and urbanizing fire-prone landscapes.

Plain Language Summary Pyrocumulonimbus wildfires (pyroCb) are extreme wildfires. They involve a coupling between the fire and the atmosphere, which drives dangerous fire conditions that result in fatalities and considerable damage. Climate change could amplify the conditions associated with pyroCb development. We use high-resolution regional climate projection data to assess future changes in the risk of pyroCb occurrence for southeastern Australia. We demonstrate that atmospheric instability and dryness is a better indicator of pyroCb development than surface fire weather conditions, with topographic roughness and vegetation type also playing roles. Coincidences of high index values of atmospheric conditions (tropospheric instability and dryness) and surface fire weather conditions (temperature, humidity, wind speed, and precipitation) associated with pyroCb development are projected to increase in frequency predominantly for November (spring) in 2060-2079 versus 1990-2009, but less so for summer. The extension of the season conducive to pyroCbs into spring is important because Australian pyroCbs are typically summer phenomena. A change in seasonality has implications for resource allocations by fire agencies. Projected changes in the conditions conducive to pyroCbs are primarily associated with increased dryness at 1.5-km altitude. These findings are relevant to the mitigation of pyroCbs, and they have implications for continued urban expansion on fire-prone landscapes.

1. Introduction

Large wildfires are global phenomena that pose significant risks to property and life, with climate change and development on fire-prone landscapes threatening to exacerbate these problems (Bowman et al., 2017). Several severe wildfires that have occurred in Australia (Field et al., 2016; Fromm et al., 2006; McRae et al., 2013), and globally (Fromm et al., 2010; Lang et al., 2014; Peterson et al., 2017), were characterized by widespread flaming areas that generated violent pyroconvection due to favorable atmospheric conditions (Sharples et al., 2016). They generated towering pyrocumulonimbus (pyroCb) storms and involved a coupling between the fire and troposphere (Potter, 2012a, 2012b). These dangerous wildfires are influenced by several factors, including the occurrence of atmospheric instability and dryness and surface fire weather conditions conducive to their development (Cunningham & Reeder, 2009; Dowdy &

Pepler, 2018). Interactions of tropospheric processes with rugged terrain can also contribute to violent pyroconvection because they facilitate the expansive flaming often associated with pyroCb development (McRae et al., 2015; Sharples, 2009). Given that the dynamic coupling of fire-atmospheric processes can contribute to pyroCb development, a greater understanding of the strong pyroconvective processes and conditions linked to pyroCb occurrence is important. However, the conditions that influence pyroCb development are not well understood and difficult to forecast (Tory et al., 2018).

The original Haines index (Haines, 1988) was designed to indicate the potential for varying degrees of lower tropospheric instability and dryness to influence wildfires. High index values, in theory, indicate that conditions are suitable for the rapid intensification of fires into pyroCbs due to decreased tropospheric stability and increased dewpoint depression. Studies that have investigated future changes in wildfire hazard for North America by examining future changes in the Haines index found increased potential for severe wildfires (Bedel et al., 2013; Luo et al., 2013; Tang et al., 2015). However, studies that investigated the Haines index in different world regions (Long, 2006; Tatli & Turkes, 2014; Winkler et al., 2007) found considerable regional variation in index values. Mills and McCaw (2010) extended the Haines index to render it more suitable for locations where high index values occur frequently. Their continuous-Haines index (C-Haines) allows for higher values than the original index. Focusing on Australia and C-Haines, the majority of the pyrocumulus events studied by Mills and McCaw (2010) coincided with very high C-Haines levels. C-Haines levels over southeastern Australia also show an increasing trend during recent decades (Sharples et al., 2016). Moreover, a reanalysis-based C-Haines climatology for 1979-2016 showed an increased risk of strong pyroconvection during spring and summer due to a combination of increasing C-Haines values and near-surface fire weather severity (Dowdy & Pepler, 2018).

Surface fire weather conditions in Australia are commonly quantified using the McArthur Forest Fire Danger Index (FFDI; Noble et al., 1980). FFDI considers surface air temperature, relative humidity, wind speed, and precipitation. Studies based on observations have shown large increases in FFDI over recent decades in southeastern Australia, with these changes partially attributable to anthropogenic influences including increasing temperatures (Dowdy, 2018). Projected future changes in wildfire incidences across Australia using FFDI calculated from climate projections (Clarke et al., 2011; Fox-Hughes et al., 2014) have generally found that FFDI increases.

Here we hypothesize that high index values of surface fire weather, estimated using FFDI, and atmospheric conditions favorable for enhanced pyroconvection estimated using the C-Haines index, are necessary for pyroCb development. We first examine whether observed pyroCbs correspond with high values of FFDI and C-Haines in southeastern Australia. We also determine how frequently pyroCbs occur on rugged versus nonrugged terrain, and within different vegetation types. We then use a regional climate projection ensemble to investigate future projected changes to the cooccurrence of high values of C-Haines and FFDI and the implications of this for the future occurrence of pyroCbs.

2. Materials and Methods

2.1. Regional Climate Models

We used an ensemble of 12 high-resolution (10-km) regional climate model (RCM) simulations over southeastern Australia to derive C-Haines and FFDI estimates for three 20-year periods: historical (1990-2009), near-future (2020-2039), and far-future (2060-79). Future simulations followed the A2 scenario from the Special Report on Emissions Scenarios (Nakićenović et al., 2000). Simulations comprised part of the New South Wales/Australian Capital Territory Regional Climate Modelling (NARCliM) project to produce regional-scale climate projections for southeastern Australia. The NARCliM ensemble representation of recent climate has been extensively evaluated (e.g., Bao et al., 2017; Cortes-Hernandez et al., 2016) and provides overall added value to the global climate model (GCM) projections (Di Luca et al., 2016).

An overview of the NARCliM experimental setup is provided here; Evans et al. (2014) provides further details. This 12-member ensemble was created by selecting four GCMs (Model for Interdisciplinary Research on Climate 3.2-medres [MIROC3.2-medres], European Centre/Hamburg version 5 [ECHAM5], Canadian Centre for Climate Modelling and Analysis version 3.1 [CCCMA3.1], and Commonwealth Scientific and Industrial Research Organisation Mark version 3.0 [CSIRO-Mk3.0]) from the 3rd Coupled

Model Intercomparison Project based on their skill in simulating the southeastern Australian climate and model independence. Outputs from these GCMs were dynamically downscaled using three configurations of the Weather Research and Forecasting (WRF) model version 3.3 (Skamarock et al., 2008). The three WRF configurations used different combinations of parameterizations for surface/planetary boundary layer, cumulus convection, and atmospheric radiation but used the same dynamical core, land surface model (Unified Noah), and subgrid-scale microphysics scheme (WDM-5; Evans et al., 2014). The three configurations were selected from a 36-member ensemble that used different physical parameterizations based on their model skill and independence (Evans et al., 2012; Ji et al., 2014).

RCM simulations were conducted using a nested approach. GCM outputs were first used as initial and lateral boundary conditions for each RCM for an outer domain covering the CORDEX-Australasia region with a quasi-regular resolution of ~50 km. The initial and lateral boundary conditions from the outer grid run were then used to drive the same RCM over an inner domain covering southeastern Australia at ~10-km resolution. Analyses focus on the inner domain only.

2.2. C-Haines and FFDI

C-Haines was calculated after Mills and McCaw (2010) and comprised summing two terms, CA and CB: CA is a stability term representing the difference between temperatures at 850 and 700 hPa; CB is a moisture term representing the dewpoint depression at 850 hPa, equal to the temperature at 850 hPa minus the dew point temperature at 850 hPa. FFDI was used to represent near-surface fire weather conditions. It was calculated following Finkele et al. (2006) using near-surface daily maximum temperature, and 0400 UTC wind speed and relative humidity, and the daily drought factor (Noble et al., 1980).

For the purposes of RCM validation, C-Haines and FFDI were obtained for the historical period (1990-2009) from a combination of reanalysis and observed data sets. We used the C-Haines data prepared using ERA-Interim reanalysis (Dee et al., 2011) by Dowdy and Pepler (2018), which had a spatial and temporal resolution of 0.75° and 6 hr. We used the FFDI data derived by Dowdy (2018), where the input variables to calculate FFDI consisted of a gridded analysis of observations from the Australian Gridded Climate Data (Jones et al., 2009) at 0.05° resolution, and wind data from National Centers for Environmental Prediction/National Center for Atmospheric Research reanalysis (Kalnay et al., 1996) quantile-matched to the operational forecast wind speeds used by the Bureau of Meteorology for the provision of guidance to fire agencies. These data were interpolated to the same 10-km resolution grid as the modeled data using inverse square distance interpolation and aggregated to daily maxima.

2.3. Relationships of Wildfires to C-Haines, FFDI, Landscape Ruggedness, and Vegetation Type

The magnitudes of observed C-Haines and FFDI values for 1990-2016 that were coincident with the dates and locations of historical wildfires for this period were assessed. The landform-type on which fires occurred was identified using the 30-m resolution slope-relief landform pattern classification of Gallant and Austin (2012). We also identified the vegetation class on which fires occurred using the 100-m resolution National Vegetation Information System (NVIS) version 5.1 (Australian Government, 2018). We examined two classes of wildfire. One class (N=40) comprised all confirmed pyroCbs that occurred in the study domain during 1990-2016. The majority of pyroCbs (70%) occurred within the state of Victoria. pyroCbs were identified using the on-going Australian PyroCb Register (McRae et al., 2015; see Table S3 in the supporting information for the April 2019 version of this register). This register relies on expert analysis of information from a wide range of direct and remote observations. These combine atmospheric impacts with plume dynamics and fire behavior to form a coherent picture of the event that is assessed to determine whether it meets or exceeds thresholds for a pyroCb (as discussed in Fromm et al., 2010). pyroCbs were identified using three principal data sources: (1) LANDSAT imagery to confirm the large, uniformly high intensity burn scars characteristic of pyroCbs; (2) MODIS hot spots, particularly to identify large patches within a fire complex where hotspots are absent, indicating the rapid burnout of fuels consistent with a blow-up event (note that hotspots for wildfires that are not pyroCbs tend to persist, as these fires take much longer to consume fuels; Figure S1 in the supporting information shows an illustration of this effect); and (3) radar data to confirm the date of occurrence. The second data set (N=166) comprised "standard wildfires" that occurred in Victoria during 1990-2016, which we define as wildfires that did not produce pyroCbs. These wildfires were a subset of the Victorian Government wildfire database (Department of Environment, 2019). This subset

comprised wildfires designated as "high accuracy" only, which denotes a positional accuracy of ≤25 m and validation of wildfire characteristics (size, etc.) using aerial and satellite imagery. Wildfires validated to this accuracy comprise 14.5% of historical wildfires in this database. They are widely distributed, occurring in inland and rural regions, as well as the more populated seaboard. Standard wildfires within this subset that coincided with pyroCbs and also within a radius of 20 km of their locations were excluded. Fires less than 10 ha in surface area were also omitted, because fires smaller than this size were likely to have been suppressed.

2.4. Future Changes in Coincidences of Elevated C-Haines and FFDI

Daily instances of C-Haines and FFDI values that both met or exceeded thresholds conducive to wildfire development at a given location were identified for the three periods. Two sets of thresholds were used: C-Haines ≥8 and FFDI ≥25 and C-Haines ≥10 and FFDI ≥50. The 95th percentile of C-Haines ranges from ~7 to ~10 depending upon location in southeastern Australia (Mills & McCaw, 2010), noting that the risk severity may vary with location, for example, depending upon topography (Winkler et al., 2007). An FFDI over 25 is considered a "very high" fire danger rating; an index over 50 presents a "severe" fire risk, resulting in a total fire ban. The monthly and seasonal means for the number of days that both C-Haines and FFDI met or exceeded their respective thresholds were calculated for each grid-cell for each period. The future changes in the ensemble mean number of days that both C-Haines and FFDI met or exceeded their respective threshold per season and month were calculated by subtracting the ensemble mean for each future period from the mean for 1990-2009. The statistical significance of projected changes in the mean number of days that C-Haines and FFDI met or exceeded the thresholds (henceforth "coincidences") as compared to the corresponding coincidences for 1990-2009 was calculated for each grid-cell using *t* tests (α=0.05) assuming equal variance. Results on ensemble mean statistical significance were separated into three classes following Tebaldi et al. (2011). Statistically insignificant areas are plotted in color. These are locations where fewer than 50% of models are significantly different as compared to the corresponding coincidences for 1990-2009. In areas of significant agreement (stippled), at least 50% of RCMs show coincidences that are significantly different to those of 1990-2009, and at least 75% of significant RCMs agree on the direction of change. Areas of significant disagreement are areas where at least 50% of RCMs are significantly different and fewer than 75% of significant models agree on change direction (though such instances were not present in our results).

3. Results

3.1. RCM Evaluation

Probability density functions (PDFs) were used to evaluate model skill in reproducing the observed/reanalysis C-Haines and FFDI distributions. The model PDFs generally fit the observed PDFs well. Occurrences of low C-Haines values within a range of 1-6 were generally underestimated by the RCMs (Figure S2). In contrast, RCMs generally overestimated C-Haines values in the middle of the observed distribution, whereas 50% of RCMs slightly underestimated very high values (>10). Occurrences of low FFDI values below ~10 were overestimated by all models as compared to the observations-based dataset, whereas occurrences of higher values (≥20) were underestimated (Figure S3).

3.2. Relationships Between C-Haines, FFDI, and pyroCbs and Standard Wildfires

Figure 1 shows the percentage of grid-cell events that occur for increments of 0.5 C-Haines and 2 FFDI during spring (September-November; SON) and summer (December-January-February; DJF) in 1990-2016 for the observed data. It also shows the C-Haines and FFDI values coincident with the date and location of historical pyroCbs and standard wildfires. The majority of pyroCbs (75%) occur within a narrow range of very high C-Haines values between 10 and 13.7 (mean [*SD*] = 11.36 [1.82], see also Text S3, Figure S4, and Table S1 in the supporting information). Conversely, over 80% of pyroCbs occur during a broad range of FFDI values between 25 and 150 (mean [*SD*] = 48.7 (30.45), see also Text S3, Figure S4, and Table S1). Moreover, the high values of C-Haines and FFDI coincident with most pyroCbs are rare grid-cell events. That is, most pyroCbs are not located within the more common grid-cell events of observed C-Haines and FFDI that correspond to the warm-colored area of Figure 1. All but two pyroCbs occur on landscapes characterized by varying degrees of ruggedness, that is, on low/rolling hills or steep hills/mountains. All but four pyroCbs occur within forest/woodland.

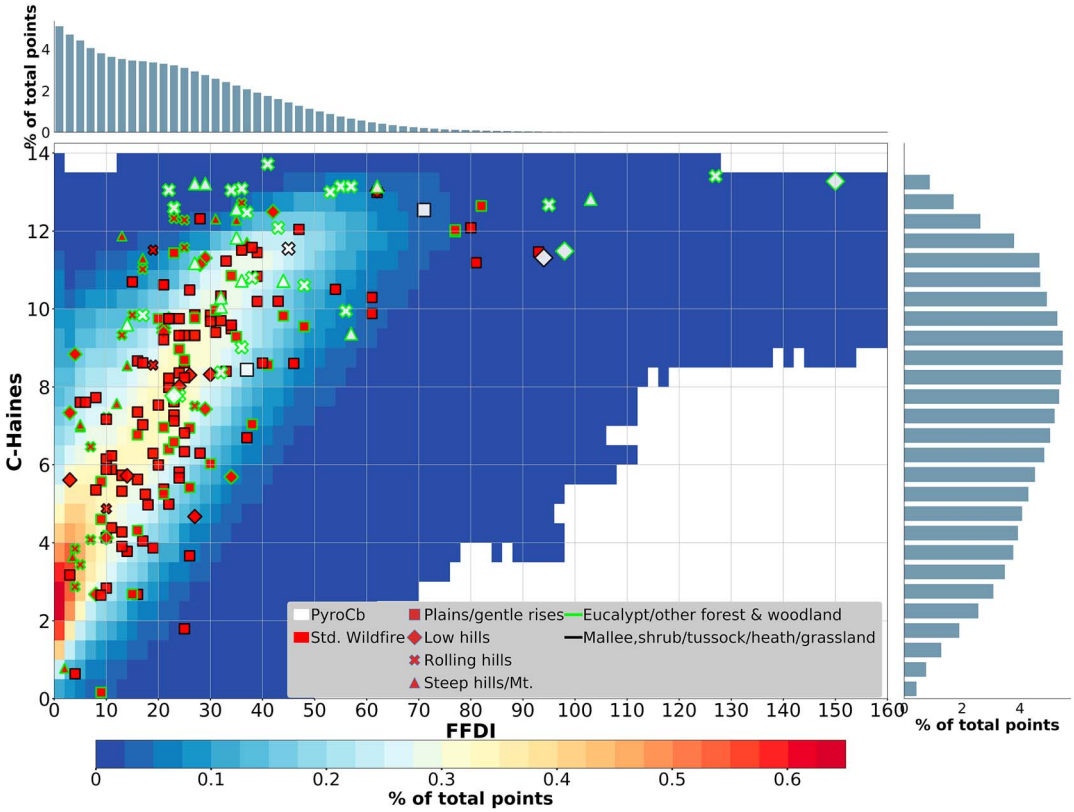

Figure 1. The percentage of grid-cell events that occurred for increments of 0.5 C-Haines and increments of 2 Forest Fire Danger Index (FFDI) during 1990-2016, and the C-Haines and FFDI values at the date and location of pyroCbs (N=40) and standard wildfires (N=166). The landform type and vegetation type on which fires occurred are also symbolized.

In contrast to the pyroCbs, most standard wildfires (76%) occur during a much broader range of C-Haines values of 2 to 10 (Figure 1) that are substantially lower on average (mean [SD] =7.84 (2.97); see also Figure S4 and Table S1). The majority of standard wildfires also occur during lower FFDI values in a smaller range of between 20 and 40 (mean [SD] =24.63 [16.6]; Figure S4 and Table S1) and over 70% occur on flat terrain. However, a minority (18%) of standard wildfires occur during C-Haines values ≥11, and over 50% of these wildfires occur on terrain that was not flat, which contrasts with the majority of standard wildfires. Repeating the analysis above using data restricted to Victoria produced similar results (Figure S5).

3.3. Projected Changes in Coincidences of Elevated C-Haines and FFDI

While the observations are largely in the state of Victoria, we now extend the analysis to all of southeast Australia. Figures 2b and 2c and 2e and 2f show projected future increases in the mean number of days that modeled FFDI and C-Haines both meet or exceed their respective target thresholds during SON, relative to the historical period (Fig 2a and 2d). There are statistically significant projected increases in the mean number of days that C-Haines and FFDI are ≥8 and ≥25, respectively, across large areas of southeastern Australia during SON in 2060-2079 versus 1990-2009 (Fig. 2c). These increases are projected to occur over areas that include agricultural regions and near urban areas. In several locations, increases are in the range of 4-5 days on average (Fig. 2c). By comparison, significant increases in coincidences of C-Haines ≥10 and FFDI ≥50 are more geographically restricted during 2060-2079 (Fig. 2f). Such changes are almost entirely absent during 2020-2039 for both sets of thresholds (Fig. 2b and 2e). Although there is also a statistically significant increase in the mean number of days that C-Haines and FFDI are ≥8 and ≥25, respectively, during summer in 2060-2079 (Fig. 3c), this increase covers a smaller area than for spring in 2060-2079 (Fig. 2c). For all periods and seasons, several areas do not show significant projected changes, particularly for the upper C-Haines and FFDI thresholds.

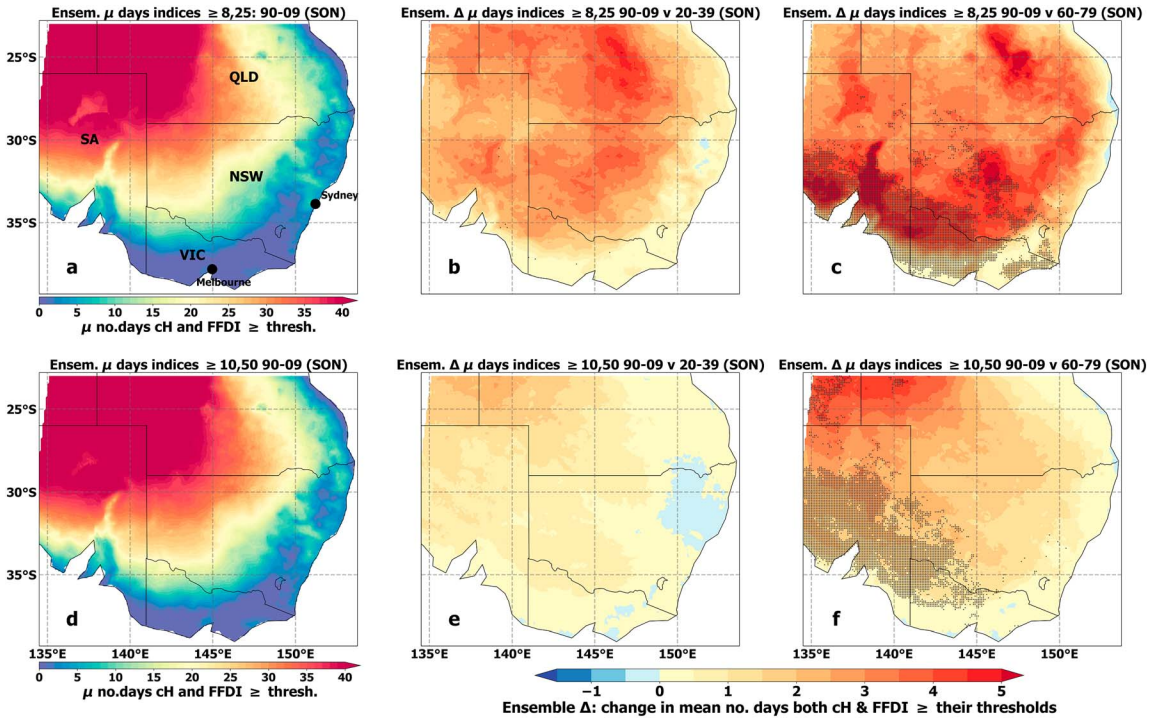

Figure 2. (a) Ensemble mean number of days that both C-Haines and FFDI ≥8 and 25, respectively, or (d) ≥10 and 50, during spring (September-October-November [SON]) for 1990-2009. QLD=Queensland; NSW=New South Wales; VIC=Victoria; SA=South Australia; (b and c) ensemble mean change in the number of days that both C-Haines and FFDI ≥ 8 and 25 respectively during SON between 1990-2009 versus 2020-2039 and 1990-2009 versus 2060-2079; (e and f) as per panels b and c but for C-Haines and FFDI ≥10 and 50, respectively. Significance stippling (b, c, e, and f): statistically insignificant areas are shown in color only. Significant agreeing areas are in color and stippled.

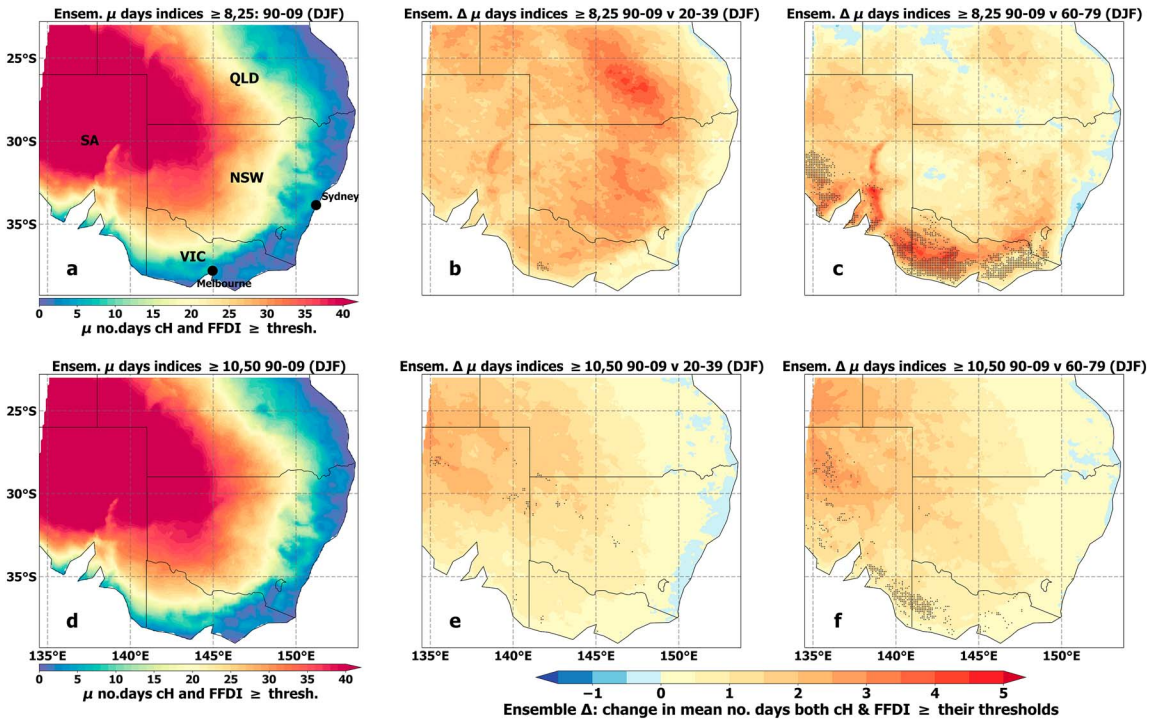

Figure 3. As per Fig. 2 but for summer (December-January-February [DJF]).

During spring, the significant projected coincident increases in C-Haines and FFDI described above occur predominantly during November (Figure S6), as opposed to during September and October (Figures S7 and S8). Similarly, the summer-time significant increase occurs mainly during December (Figure S9) as opposed to during January and February (not shown).

Future changes in coincident elevated C-Haines and FFDI values projected by individual RCMs during spring are discussed in Text S5 and Figure S10. Additionally, projected changes in the number of grid-cell events that occur for increments of 0.5 C-Haines and 2 FFDI simulated by the ensemble in 2060-2079 relative to 1990-2009 are discussed in Text S6 and Figure S11.

4. Discussion

Observed pyroCbs predominantly occur during high C-Haines values between 10 and 13.7 but over a wide range of surface fire weather conditions between 25 and 150. These results indicate that atmospheric instability and dryness is a better indicator of pyroCb development than surface fire weather conditions. Standard wildfires generally occurred during lower C-Haines values (2 to 10), but during a similar range of FFDI values.

Over 90% of pyroCbs occurred on rugged landscapes, whereas over 70% of standard wildfires occurred on plains. This is consistent with previous findings that interactions between winds and rugged terrain can be conducive to the expansive flaming zones associated with pyroCb development and increased wildfire severity (Sharples, 2009). Consequently, the danger posed by a given C-Haines value varies as a function of topography: a C-Haines of 10 does not pose the same level of risk on plains compared to hilly terrain. This has a clear implication for how fire-management agencies appraise the risk of dangerous wildfires given projected C-Haines levels.

There was a significant increase in the mean number of days with conditions conducive to pyroCb development during the spring and summer of 2060-2079 relative to 1990-2009. Given the potential roles of ruggedness and vegetation type in pyroCb development, we note that 24.4% of grid-cells showing a significant change during SON in 2060-79 are also characterized by varying degrees of ruggedness and 12.5% are forest/woodland. Increases in days with high values of both C-Haines and FFDI occurred predominantly during November (end of spring) and December (start of summer), indicating an increased risk of pyroCbs during these months. However, this projected increase covered a much smaller portion of southeastern Australia during the summer than spring. pyroCbs observed to date were typically summer phenomena (over 90% of pyroCbs assessed occurred during summer, the remainder during spring). This suggests that the portion of the year prone to pyroCb occurrence could extend into spring, with implications for their mitigation and management. Previously, an observations and reanalysis-based study for 1979-2016 showed an increased risk of strong pyroconvection for southeastern Australia during both spring and summer (Dowdy & Pepler, 2018). Here the significant projected change in cooccurrences of elevated C-Haines and FFDI was near some heavily populated regions. This is an important finding from a policy perspective, as continued urban expansion in these regions risks increasing exposure to atmospheric and surface fire weather conditions that are conducive to these dangerous wildfires. However, interpretation of these results must be tempered by the observation that many RCMs overestimated C-Haines occurrences in the middle of the observed distribution by a small degree, whereas 50% of RCMs underestimated occurrences of very high C-Haines values >10 (Figures S2 and S3).

A minority of standard wildfires occurred during C-Haines values ≥11 and on rugged terrain. Explanations why these wildfires did not develop into pyroCbs include the absence of a mechanism for expansive flaming, agencies having succeeded in fire suppression before development of a strong convective plume, and/or light-moderate rain hindering fire intensification. See Table S2 and Figures S12-S19 for further potential explanations why these wildfires did not develop into pyroCbs.

In addition to the analyses described above, we investigated the factors linked to the projected increases in C-Haines. The components of C-Haines (CA and CB) increase by different degrees in 2060-2079 relative to 1990-2009. On average, the magnitudes of CA scores increase by a very small amount over the majority of the region during November in 2060-2079 relative to 1990-2009 (Fig. 4a). In contrast, CB scores increase by between 0.2 and 0.5 over most regions during November in 2060-2079 (Fig. 4b). This increase was

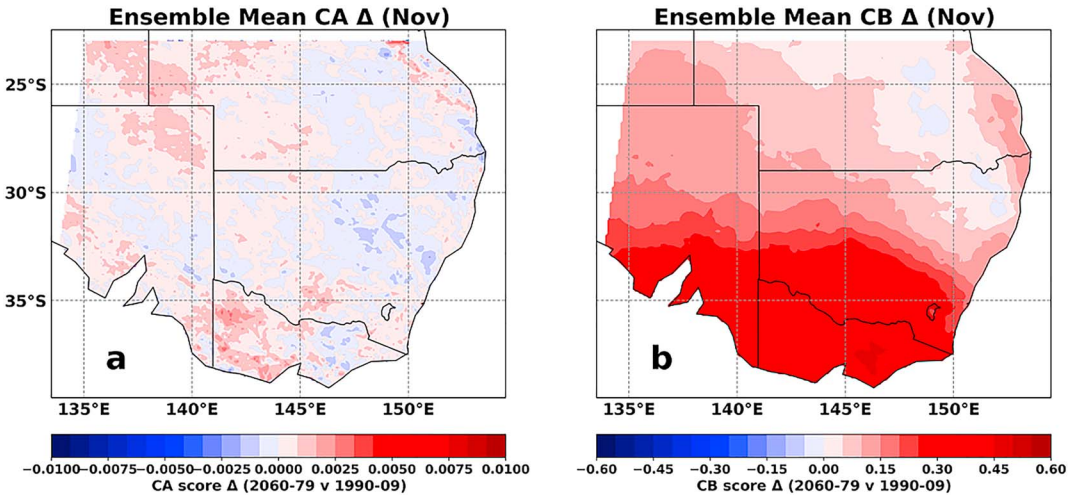

Figure 4. (a) Projected changes in ensemble daily mean CA in 2060-2079 versus 1990-2009 during November using CA scores ≥5. (b) Projected changes in ensemble daily mean CB (all scores).

largest over the southern region where the significant increase in coincidences of elevated C-Haines and FFDI was observed. The results for CA and CB were similar during the other periods considered (December, SON, and DJF). The projected changes in mean number of days that CA and CB met or exceeded a threshold of 5 showed a similar pattern of results. Repeating the analyses only for grid-cells designated as rugged (i.e., not plains or gentle rises) and as forest/woodland produced similar results to the above. Clarke and Evans (2018) provide further analysis of projected changes in the component variables of FFDI.

Although small in magnitude, any projected increase in the CA term would likely contribute to an increased risk of strong pyroconvection. The increase in the CB score in 2060-2079 means that air at 850 hPa is projected to be drier as represented by a larger difference between the temperature and the dewpoint at 850 hPa (i.e., increased dewpoint depression at 850 hPa). This is a potentially dangerous scenario, because if this dry air is returned to the surface via convective mixing, it could lead to increased levels of fire behavior and rates of spread (Mills, 2008a, 2008b). Such fires would be difficult to control and could cause considerable damage (McRae & Sharples, 2011). A mixing-down of dry, hot winds to the surface occurred during the catastrophic Black Saturday Fires in Australia on 7 February 2009 (Cruz et al., 2012).

An additional risk presented by very high C-Haines values is the previous observation that periods of high C-Haines coincided with weak overnight relative humidity recovery (Mills & McCaw, 2010). The cooccurrence and persistence of both of these phenomena could lead to a situation where there are both dry surface fuels and atmospheric conditions conducive to strong pyroconvection. The potential for a causal link between occurrences of extremely high C-Haines values and weak overnight relative humidity recovery merits further investigation.

5. Conclusions

This study yielded three main findings: (1) observed pyroCbs predominantly occur on rugged, forest/woodland landscapes during high levels of tropospheric instability and dryness but over a wide range of surface fire weather conditions; (2) a significant increase in the mean number of days that both C-Haines and FFDI meet or exceed thresholds conducive to pyroCb development is projected for November in 2060-2079 relative to 1990-2009, and less so for December; and (3) the locations where these changes are projected to occur are identified. The extension of the season conducive to pyroCbs into spring is important because currently Australian pyroCbs are typically summer phenomena and a change in seasonality has implications for resource allocations of fire agencies. Moreover, projected increases in C-Haines values are linked to decreased 850-hPa humidity (associated with increased dewpoint depression) during SON in 2060-2079. Together, these findings are relevant to agencies involved in climate impact adaptation, and the planning

for and management of dangerous wildfires in Australia and potentially various regions globally. This will increase the preparedness requirements of society to mitigate the consequences of these dangerous conditions, and has implications for urban expansion on fire-prone landscapes.

Acknowledgments
The authors declare that they have no conflict of interest. pyroCb data are available in Table S3. Climate projection data are available from the AdaptNSW repository: https://climatechange.environment.nsw.gov.au/Climate-projections-for-NSW/Download-datasets. Logistical support was provided by the Climate Change Research Centre at the University of New South Wales and by the National Computing Infrastructure National Facility at Australian National University. This project is supported through funding from the Earth Systems and Climate Change Hub of the Australian Government's National Environmental Science Programme and the NSW government Office of Environment and Heritage. We thank Tim Wells of the Victorian Country Fire Authority for providing data on wildfires. We thank Robert Colman, Mika Peace and Kevin Tory at the Bureau of Meteorology for providing feedback on the manuscript.

References

Australian Government (2018). National Vegetation Information System V5.1. Department of the Environment and Energy

Bao, J. W., Sherwood, S. C., Alexander, L. V., & Evans, J. P. (2017). Future increases in extreme precipitation exceed observed scaling rates. *Nature Climate Change*, *7*(2), 128–132. https://doi.org/10.1038/nclimate3201

Bedel, A. P., Mote, T. L., & Goodrick, S. L. (2013). Climate change and associated fire potential for the south-eastern United States in the 21st century. *International Journal of Wildland Fire*, *22*(8), 1034–1043. https://doi.org/10.1071/WF13018

Bowman, D. M. J. S., Williamson, G. J., Abatzoglou, J. T., Kolden, C. A., Cochrane, M. A., & Smith, A. M. S. (2017). Human exposure and sensitivity to globally extreme wildfire events. *Nature Ecology & Evolution*, *1*(3), 0058. https://doi.org/10.1038/s41559-016-0058

Clarke, H., & Evans, J. P. (2018). Exploring the future change space for fire weather in southeast Australia. *Theoretical and Applied Climatology*, *136*(1–2), 513–527. https://doi.org/10.1007/s00704-018-2507-4

Clarke, H., Smith, P. L., & Pitman, A. J. (2011). Regional signatures of future fire weather over eastern Australia from global climate models. *International Journal of Wildland Fire*, *20*(4), 550–562. https://doi.org/10.1071/WF10070

Cortes-Hernandez, V. E., Zheng, F. F., Evans, J., Lambert, M., Sharma, A., & Westra, S. (2016). Evaluating regional climate models for simulating sub-daily rainfall extremes. *Climate Dynamics*, *47*(5-6), 1613–1628. https://doi.org/10.1007/s00382-015-2923-4

Cruz, M. G., Sullivan, A. L., Gould, J. S., Sims, N. C., Bannister, A. J., Hollis, J. J., & Hurley, R. J. (2012). Anatomy of a catastrophic wildfire: The Black Saturday Kilmore East fire in Victoria, Australia. *Forest Ecology and Management*, *284*, 269–285. https://doi.org/10.1016/j.foreco.2012.02.035

Cunningham, P., & Reeder, M. J. (2009). Severe convective storms initiated by intense wildfires: Numerical simulations of pyro-convection and pyro-tornadogenesis. *Geophysical Research Letters*, *36*, L12812. https://doi.org/10.1029/2009gl039262

Dee, D. P., Uppala, S. M., Simmons, A. J., Berrisford, P., Poli, P., Kobayashi, S., et al. (2011). The ERA-Interim reanalysis: Configuration and performance of the data assimilation system. *Quarterly Journal of the Royal Meteorological Society*, *137*(656), 553–597. https://doi.org/10.1002/qj.828

Department of Environment, Land, Water & Planning (2019). *Fire history overlay of most recent fires (Anzlic Id: ANZVI0803004774)*. Australia: Victorian Government.

Di Luca, A., Argueso, D., Evans, J. P., de Elia, R., & Laprise, R. (2016). Quantifying the overall added value of dynamical downscaling and the contribution from different spatial scales. *Journal of Geophysical Research: Atmospheres*, *121*, 1575–1590. https://doi.org/10.1002/2015JD024009

Dowdy, A. J. (2018). Climatological Variability of Fire Weather in Australia. *Journal of Applied Meteorology and Climatology*, *57*(2), 221–234. https://doi.org/10.1175/JAMC-D-17-0167.1

Dowdy, A. J., & Pepler, A. (2018). Pyroconvection risk in Australia: Climatological changes in atmospheric stability and surface fire weather conditions. *Geophysical Research Letters*, *45*, 2005–2013. https://doi.org/10.1002/2017GL076654

Evans, J. P., Ekström, M., & Ji, F. (2012). Evaluating the performance of a WRF physics ensemble over South-East Australia. *Climate Dynamics*, *39*(6), 1241–1258. https://doi.org/10.1007/s00382-011-1244-5

Evans, J. P., Ji, F., Lee, C., Smith, P., Argüeso, D., & Fita, L. (2014). Design of a regional climate modelling projection ensemble experiment - NARCliM. *Geoscientific Model Development*, *7*(2), 621–629. https://doi.org/10.5194/gmd-7-621-2014

Field, R. D., Luo, M., Fromm, M., Voulgarakis, A., Mangeon, S., & Worden, J. (2016). Simulating the Black Saturday 2009 smoke plume with an interactive composition-climate model: Sensitivity to emissions amount, timing, and injection height. *Journal of Geophysical Research: Atmospheres*, *121*, 4296–4316. https://doi.org/10.1002/2015JD024343

Finkele, K., Mills, G. A., Beard, G., & Jones, D. A. (2006). National gridded drought factors and comparison of two soil moisture deficit formulations used in prediction of Forest Fire Danger Index in Australia. *Australian Meteorological Magazine*, *55*(3), 183–197.

Fox-Hughes, P., Harris, R., Lee, G., Grose, M., & Bindoff, N. (2014). Future fire danger climatology for Tasmania, Australia, using a dynamically downscaled regional climate model. *International Journal of Wildland Fire*, *23*(3), 309–321. https://doi.org/10.1071/WF13126

Fromm, M., Lindsey, D. T., Servranckx, R., Yue, G., Trickl, T., Sica, R., et al. (2010). The untold story of pyrocumulonimbus. *Bulletin of the American Meteorological Society*, *91*(9), 1193–1210. https://doi.org/10.1175/2010BAMS3004.1

Fromm, M., Tupper, A., Rosenfeld, D., Servranckx, R., & McRae, R. (2006). Violent pyro-convective storm devastates Australia's capital and pollutes the stratosphere. *Geophysical Research Letters*, *33*, L05815. https://doi.org/10.1029/2005gl025161

Gallant, J., & Austin, J. (2012). Slope relief classification derived from 1" SRTM DEM-S. v3. CSIRO. Data Collection. Australian Government

Haines, D. (1988). A lower atmosphere severity index for wildland fires. *National Weather Digest*, *13*, 23–27.

Ji, F., Ekström, M., Evans, J. P., & Teng, J. (2014). Evaluating rainfall patterns using physics scheme ensembles from a regional atmospheric model. *Theoretical and Applied Climatology*, *115*(1-2), 297–304. https://doi.org/10.1007/s00704-013-0904-2

Jones, D. A., Wang, W., & Fawcett, R. (2009). High-quality spatial climate data-sets for Australia. *Australian Meteorological and Oceanographic Journal*, *58*(04), 233–248. https://doi.org/10.22499/2.5804.003

Kalnay, E., Kanamitsu, M., Kistler, R., Collins, W., Deaven, D., Gandin, L., et al. (1996). The NCEP/NCAR 40-year reanalysis project. *Bulletin of the American Meteorological Society*, *77*(3), 437–471. https://doi.org/10.1175/1520-0477(1996)077<0437:TNYRP>2.0.CO;2

Lang, T. J., Rutledge, S. A., Dolan, B., Krehbiel, P., Rison, W., & Lindsey, D. T. (2014). Lightning in wildfire smoke plumes observed in Colorado during summer 2012. *Monthly Weather Review*, *142*(2), 489–507. https://doi.org/10.1175/MWR-D-13-00184.1

Long, M. (2006). A climatology of extreme fire weather days in Victoria. *Australian Meteorological Magazine*, *55*(1), 3–18.

Luo, L. F., Tang, Y., Zhong, S. Y., Bian, X. D., & Heilman, W. E. (2013). Will future climate favor more erratic wildfires in the Western United States? *Journal of Applied Meteorology and Climatology*, *52*(11), 2410–2417. https://doi.org/10.1175/JAMC-D-12-0317.1

McRae, R., & Sharples, J. (2011). A conceptual framework for assessing the risk posed by extreme bushfires. *Australian Journal of Emergency Management*, *26*(2), 49–55.

McRae, R. H. D., Sharples, J. J., & Fromm, M. (2015). Linking local wildfire dynamics to pyroCb development. *Natural Hazards and Earth System Sciences*, *15*(3), 417–428. https://doi.org/10.5194/nhess-15-417-2015

McRae, R. H. D., Sharples, J. J., Wilkes, S. R., & Walker, A. (2013). An Australian pyro-tornadogenesis event. *Natural Hazards*, *65*(3), 1801–1811. https://doi.org/10.1007/s11069-012-0443-7

Mills, G. A. (2008a). Abrupt surface drying and fire weather Part 1: Overview and case study of the South Australian fires of 11 January 2005. *Australian Meteorological Magazine*, *57*(4), 299–309.

Mills, G. A. (2008b). Abrupt surface drying and fire weather. Part 2: A preliminary synoptic climatology in the forested areas of southern Australia. *Australian Meteorological Magazine*, *57*(4), 311–328.

Mills, G. A., & McCaw, L. (2010). *Atmospheric stability environments and fire weather in Australia—Extending the Haines Index*. Australia: Australian Government, Bureau of Meteorology.

Nakićenović, N., Alcamo, J., Davis, G., de Vries, B., Fenhann, J., Gaffin, S., et al. (2000). *IPCC Special report on emissions scenarios (SRES)*. UK: Cambridge University Press.

Noble, I. R., Bary, G. A. V., & Gill, A. M. (1980). McArthur fire-danger meters expressed as equations. *Australian Journal of Ecology*, *5*(2), 201–203. https://doi.org/10.1111/j.1442-9993.1980.tb01243.x

Peterson, D. A., Hyer, E. J., Campbell, J. R., Solbrig, J. E., & Fromm, M. D. (2017). A Conceptual model for development of intense pyrocumulonimbus in Western North America. *Monthly Weather Review*, *145*(6), 2235–2255. https://doi.org/10.1175/MWR-D-16-0232.1

Potter, B. E. (2012a). Atmospheric interactions with wildland fire behaviour—I. Basic surface interactions, vertical profiles and synoptic structures. *International Journal of Wildland Fire*, *21*(7), 779–801. https://doi.org/10.1071/WF11128

Potter, B. E. (2012b). Atmospheric interactions with wildland fire behaviour—II. Plume and vortex dynamics. *International Journal of Wildland Fire*, *21*(7), 802–817. https://doi.org/10.1071/WF11129

Sharples, J. J. (2009). An overview of mountain meteorological effects relevant to fire behaviour and bushfire risk. *International Journal of Wildland Fire*, *18*(7), 737–754. https://doi.org/10.1071/WF08041

Sharples, J. J., Cary, G. J., Fox-Hughes, P., Mooney, S., Evans, J. P., Fletcher, M. S., et al. (2016). Natural hazards in Australia: Extreme bushfire. *Climatic Change*, *139*(1), 85–99. https://doi.org/10.1007/s10584-016-1811-1

Skamarock, W. C., Klemp, J. B., Dudhia, J., Gill, D. O., Barker, D. M., Wang, W., & Powers, J. G. (2008). A description of the Advanced Research WRF Version 3. NCAR Tech Note NCAR/TN-475+STR. NCAR. Retrieved from Boulder, CO:

Tang, Y., Zhong, S. Y., Luo, L. F., Bian, X. D., Heilman, W. E., & Winkler, J. (2015). The potential impact of regional climate change on fire weather in the United States. *Annals of the Association of American Geographers*, *105*(1), 1–21. https://doi.org/10.1080/00045608.2014.968892

Tatli, H., & Turkes, M. (2014). Climatological evaluation of Haines forest fire weather index over the Mediterranean Basin. *Meteorological Applications*, *21*(3), 545–552. https://doi.org/10.1002/met.1367

Tebaldi, C., Arblaster, J. M., & Knutti, R. (2011). Mapping model agreement on future climate projections. *Geophysical Research Letters*, *38*, L23701. https://doi.org/10.1029/2011GL049863

Tory, K. J., Thurston, W., & Kepert, J. D. (2018). Thermodynamics of pyrocumulus: A Conceptual Study. *Monthly Weather Review*, *146*(8), 2579–2598. https://doi.org/10.1175/MWR-D-17-0377.1

Winkler, J. A., Potter, B. E., Wilhelm, D. F., Shadbolt, R. P., Piromsopa, K., & Bian, X. D. (2007). Climatological and statistical characteristics of the Haines Index for North America. *International Journal of Wildland Fire*, *16*(2), 139–152. https://doi.org/10.1071/WF06086